JOURNAL OF APPLIED ELECTROCHEMISTRY 1 (1971) 79–90

Parametric study of the anode of an implantable biological fuel cell

A. J. APPLEBY, D. Y. C. NG,* H. WEINSTEIN†

Received 13 October 1970, revised MS received 31 December 1970

In this paper, electrochemical oxidation of glucose at the concentration level present in human venous plasma is discussed, with the object of determining the feasibility of constructing an implantable fuel cell for powering a prosthetic heart. The model anode considered consists of a diffusing membrane, to prevent blood contact, backed by a porous electrode structure. The latter is assumed to consist of parallel tubular pores of length equal to the electrode thickness. The variation of membrane and electrode parameters and rate constants for glucose oxidation are considered as functions of reaction order and oxidation product under different flow conditions. It is shown that the least optimistic case, oxidation of glucose only to gluconic acid, is apparently marginally feasible.

Introduction

In the proposed use of prosthetic hearts as a possible therapy for cardiac patients, individual cases may require either temporary-assist devices to allow the natural heart to recover or implantable partial- or total-replacement mechanical hearts. In the latter cases, an implantable power source is needed to drive the heart pump [1]. A totally implantable power source that requires no recharging or replenishment is the ultimate goal. A number of thermo-electric and heat engines which rely on a high-temperature radioactive isotope heat source have been considered [2]. In view of the Carnot limitation inherent in these machines, the most interesting device so far proposed is an implanted fuel cell that uses metabolic intermediates present in the blood as its fuel and oxygen as its oxidant. In addition to the often quoted advantages of high thermal efficiency, lack of mechanical parts, etc., the fuel cell would be completely self-sufficient in that, like the natural heart, it draws its continuous supply of energy from the blood.

The special conditions under which an implantable fuel cell will have to operate pose a number of new problems and revive some old ones. The electrolyte of the cell is virtually restricted to a plasma ultrafiltrate (0·154 molar solution containing Cl^- ion buffered by bicarbonate at a pH of 7·4). Neutral buffered electrolytes suffer from mass transport problems that result in inadequate pH control at electrodes compared with strong acid or alkaline solutions [3]. In several designs, this problem is eliminated by the use of an encapsulated acid or alkaline electrolyte [4, 5].

The nominal oxygen content in blood is high. However, most of the oxygen (up to 97%) is bound up in the arterial haemoglobin. Solubility in plasma under the arterial partial pressure (0·125 atm.) is only 10^{-4} molar, whereas the total oxidizable metabolic intermediate concentration is about 10^{-2} molar. The possibility of finding an electrocatalyst that will selectively reduce small amounts of oxygen without simultaneous oxidation of excess organic material seems remote [6]. Another approach is the use of a deoxygenator constructed with dual-porosity hydrophobic membranes to separate gaseous oxygen from blood [7]. Very large diffusion areas are necessary. Preliminary designs showed that, under the most favourable conditions, the deoxygenator will have large numbers of tubes of very small diameter [7]. Such a configuration may not be feasible because of

* Institute of Gas Technology, Chicago, Illinois, U.S.A.
† Chemical Engineering Department, Illinois Institute of Technology, Chicago, Illinois, U.S.A.

possible blood haemolysis and clotting and because of the very low exit oxygen partial pressure (~0·01 atm.). The alternative is to supply air percutaneously to the fuel cell cathode [8] when the available cathode oxygen partial pressure is about 0·21 atm. Existing diffusion electrode technology would be transferable to this development. Many design and surgical problems of the direct air system remain, however, for future investigation, and will not be further considered here.

At the anode of the implantable fuel cell the glucose and other oxidizable organics are dissolved in the blood. To avoid poisoning of the anode catalyst by proteins and other large molecules,* the electrode should be protected by a suitable membrane, which must be compatible with blood. The dilute solution of glucose in blood ultrafiltrate ($0{\cdot}5 \times 10^{-5}$ molar) is transported through the membrane to the reaction sites on the electrode. This paper will explore parametrically the mass transport of the dissolved glucose fuel through the membrane and within a porous electrode under diffusion and forced-convection with diffusion. Only glucose is considered to be oxidized at the anode. In addition, the oxidation is assumed to proceed from glucose to gluconic acid only, yielding two electrons in the process.

Physical design consideration of the fuel cell anode

The fuel cell anode should be located in the venous circulation where the dissolved oxygen level is at a minimum. It must also be located in a region of high systolic blood pressure if forced perfusion of the electrode structure is desired. The left arterial side of the artificial heart pump must develop a head of at least 80 mmHg to perfuse the systemic circulation. It is reasonable to suppose that the design of a prosthetic heart would be simplified if both sides developed the same pressure head, which is not the case with the natural organ. From these considerations, the most suitable location for the anode is between the right ventricle of the artificial pump and the pulmonary artery. The pump and anode can be designed integrally such that the pressure just upstream of the lungs is physiologically correct.

To obtain as high a plasma flow as possible through the electrode structure, the anode should be designed so that the plasma passes through just one thickness of membrane while flowing from the pump to the pulmonary artery. One way to effect this would have the blood stream leaving the heart enter a reservoir adjoining the membrane. Some of the plasma would then be forced through the membrane, the remaining blood being throttled down to pulmonary artery pressure. The plasma stream could then flow from the electrode through a check valve to a second reservoir, where it would meet the throttled stream. The reconstituted venous flow would then enter the pulmonary artery.

For the alternative case, where glucose is transferred to the electrode by molecular diffusion alone, the anode might be located upstream of the right artificial ventricle and the two halves of the artificial heart would pump at different pressure heads.

Electrochemistry of glucose oxidation

Electrodic oxidation of carbohydrates has been reported in acid and alkaline solution by Bockris *et al.* [9], and in neutral saline solution by Rao and Drake [10]. The latter authors specifically studied glucose oxidation in a phosphate buffer isotonic with human plasma at pH 7·4. In their experiments, glucose in comparatively high concentration was oxidized at platinum electrodes in a potential range close to the reversible potential for the reaction [11]:

$$(C_6H_{12}O_6)_{aq} + 6H_2O \rightleftharpoons 6CO_{2g} + 24H^+ + 24e^- \qquad (1)$$

E_0 calc. $-0{\cdot}015$ mV HRE*

There is considerable evidence that under the above conditions the primary reaction product is gluconic acid, $CH_2OH\ (CHOH)_4COOH$, after a 2-electron oxidation of the aldehyde group of glucose. The E_0 for the aldehyde group oxidation alone is $+0{\cdot}15$ mV HRE [12]. In the range of potential between 50 and 400 mV HRE a time-dependent decay of electrode activity occurs, which increases with applied current

* The poisoning effects of all the substances dissolved in blood have not yet been evaluated.

* The symbol HRE throughout this paper refers to the 1 atm H_2 electrode in the same solution.

density and with lower electrode specific area [13]. For high-area black electrodes a steady state is eventually reached, which is discussed specifically for Pt-black electrodes in previous publications [14].

At this steady state, electrodes have open-circuit potentials about +300 mV HRE (−150 mV SHE at pH 7·4) and there is considerable evidence of simultaneous oxidation of gluconic acid [14]. It has also been shown that much more efficient oxidation of certain other blood components can be attained (in particular, glucosamine) [14]. In this situation there is negligible decay from initial open-circuit potentials, which are close to the hydrogen electrode potential in the same solution. These electrodes are thus capable of producing the same current density at an overall cell voltage some 300 mV higher than glucose. Free glucosamine, however, is not present in the blood, and an enzyme would be required in the membrane wall to break down the glucosamine-containing mucopolysaccharides and glycoproteins. Consequently, while this is a possibility, the current discussion will be restricted to glucose oxidation.

Glucose oxidation kinetics

We can write a rate equation for glucose oxidation in the form:

$$\vec{i} = nF\vec{k}[C_A]^m \, e^{f(V)/RT} \qquad (2)$$

where n is the number of electrons available from the oxidation of 1 molecule of glucose. It is important to remember that n is probably a complex function of V (potential) and that $n \simeq 2$ at potentials close to the initial open-circuit value on freshly prepared platinum electrodes ($\simeq 50$ mV HRE), rising to higher values at higher potentials. The maximum theoretical value of n is 24 for the complete oxidation. In the above equation $\vec{k}$ represents the specific rate constant for oxidation at $V = 0$. C_A is the local glucose concentration at the electrode, and m is the chemical reaction order for oxidation (i.e. the order at constant potential). Instead of a simple transfer coefficient dependence of log i on V, the exponential f(V) term has been included to account for poisoning effects. These may be defined as time-dependent changes in potential at constant current density, so that a complex nonlinear steady-state V-log i relationship results. Under final steady-state conditions (at high potential) a Tafel slope of about $2RT/F$ occurs for carbohydrate oxidation [13, 14]. Consequently, a more realistic rate equation might be written

$$\vec{i} = nF\vec{k}(V,t)[C_A]^m \, e^{\alpha FV/RT} \qquad (3)$$

where $\alpha \simeq 1/2$ and $k(V, t)$ is a potential and time-dependent rate constant that tends to constant values at $t \to \infty$, at least for small values of i. The values of i that will allow steady-state development of V at reasonable overpotentials are markedly substrate-dependent. It has been shown that Pt-Ru alloys and rhodium are more effective in this respect than platinum [13]. Similar increased effectiveness with Pt-Ru alloys has been noted for hydrocarbon and methanol oxidation in other electrolytes [15].

The reaction order for glucose oxidation has been shown previously to be low [13], and in this respect the reaction also resembles methanol, ethylene, and other organic oxidation reactions [15, 16], where very low or even negative orders have been observed. In view of the complexity of the reaction, a simplified rate concept has been introduced into the present work.

The maximum current density attainable on smooth catalyst electrodes that did not lead to excessive initial poisoning was of the order of 5×10^{-6} A cm^2 on rhodium electrodes at 37°C in Ringer's phosphate buffer solution containing physiological strength (0·005 molar) glucose [13]. On black electrodes lower current densities based on true area caused poisoning. This is attributed to diffusion limitations in the electrode structure. However, results expressed on a projected area basis for black electrodes were appreciably better than those for smooth catalyst surfaces.

A conservative upper limit for i is thus taken to be 2×10^{-6} A/cm^2 of real electrode area, which for a porous electrode structure consisting of microcrystallite noble metal black particles will represent true current densities that are appreciably lower.

Thus, under physiological conditions

$$nF\vec{k}(V,t)[C_{A_0}]^m \, e^{\alpha FV/RT} \simeq 2 \times 10^{-6} \text{ max.} \qquad (4)$$

and

$$\vec{k}(V,t)[C_{A_0}]^m e^{\alpha FV/RT} = k_s[C_{A_0}]^m = \\ = \frac{2}{n} \times 10^{-11} \text{ mol/cm}^2\text{/s} \quad (5)$$

where C_{A_0} is the initial bulk blood glucose concentration. This value of the reaction surface rate constant is used as the basic figure in the design calculation.

In view of the low experimental reaction order for glucose oxidation, a nominal zero-order reaction is considered in the calculations, with certain key results reworked for a first-order case to see the effects of changing this parameter.

It is assumed above that a final potential of the glucose electrode of about 400 mV HRE at this current density will be attainable, as noted previously for steady-state black electrodes [14].

Thus for air electrode polarizations of about 350 mV at the low current densities encountered, the overall cell potential will be about 450 mV, which is a reasonable goal for a practical unit. For a 4·5 W fuel cell, a total current of 10 A will thus be required.

Parametric calculations

Model description

The idealized physical model of the electrode used for the calculations is that of a membrane of thickness t, and pore size r_m, backed by an electrode structure. The electrode structure is assumed to be made up of parallel pores of radius r_p, and length, l, arranged perpendicular to the membrane. The total thickness of the electrode is $t+l$. This is illustrated in Fig. 1.

The membrane-electrode structure is assumed to sit between two fluid reservoirs of constant glucose concentration. The reservoir on the membrane side contains venous blood with a glucose concentration of $0{\cdot}50 \times 10^{-5}$ mol/cc.

The reservoir behind the electrode contains plasma with a nominal glucose concentration 20% that of the venous blood. Glucose diffuses through the membrane because of the concentration gradient, which is maintained by the reaction in the electrode. If a pressure is applied

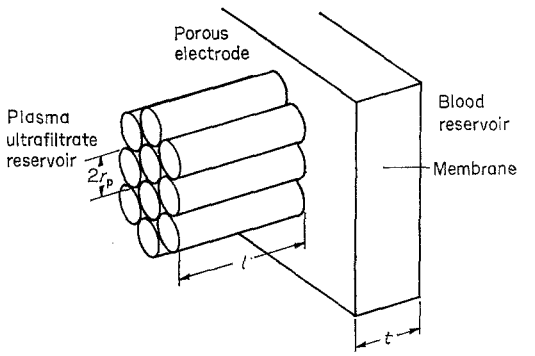

Fig. 1. Schematic membrane-electrode configuration.

across the structure, plasma is filtered through the membrane and the total glucose flux is then the sum of the diffusive flux and the convective flux.

The glucose flow into the pore structure is treated in three alternative ways:

Case I. There is no pressure differential across the anode, and glucose enters the anode by diffusion alone. The diffusion boundary layer at the blood-membrane interface is neglected.

Case II. It is assumed that a pressure differential is imposed across the anode and the glucose is brought into the pores by the resultant flow alone. This case, though unrealistic, gives an upper limit on area.

Case III. A pressure differential is applied across the anode to give a combined diffusion and convection flux. Again, the blood-membrane boundary layer is neglected, which is reasonable in a diffusion plus convection case, for sufficiently high Peclet numbers.

The overall rate of reaction of glucose can be expressed as $k_s C_A^m$, where m is considerably less than 1. In the interests of simplicity it was assumed the reaction was of zero order for all the calculations. However, several key calculations were repeated for the first-order reaction case to assess the effect of reaction order on the results.

Some basic assumptions and design criteria are listed below.

1. The power output of the fuel cell is 4·5 W delivered at 0·450 V. Faraday's law gives a corresponding glucose consumption, G, of 5×10^{-5} mol/s. This assumes that the oxida-

tion of glucose occurs only to the extent of delivering two electrons per molecule, as discussed in the previous section.

2. The membrane is assumed to be 15 μm thick, with a porosity of 50% and a pore size of 50 Å. This pore size is small enough to prevent the passage of protein molecules and yet is sufficiently large to permit the effective diffusion coefficient for glucose through the membrane to be 70% of the value in plasma [17]. For the cases of forced flow through the anode (Cases II and III), a range of membrane filtration coefficients is considered: 0·35–35·0 $\times 10^{-6}$ cc/cm^2/cm H_2O/s. The lower limit of this range corresponds to currently available commercial collodion and cellulose acetate membranes [17]. The upper limit corresponds to an idealized membrane which, if it could be developed, would not be a limiting factor in the design of the electrode.*

3. The pressure drop for the forced-flow cases (Cases II and III) is taken to be 50 mm Hg. This corresponds to a reasonable proportion of the design value of the pressure head for the heart pump. All the pressure drop is assumed to take place in the membrane for ease of calculation. Rate of flow of plasma through the membrane (U_m) values are calculated from the filtration coefficients using this value of the pressure drop.

4. The area-based rate for a zero-order reaction is taken as $k_s[C_{A_0}]^m = 10^{-11}$ mol/cm^2/s for $m = 0$ and $n = 2$. For the case of a first-order reaction the rate expression is taken to be

$$k_s = 10^{-11}\, C_A/C_{A_0}$$

where C_{A_0} is the venous blood glucose concentration. The volume-based rate constant is obtained from

$$k_v = \frac{2k_s}{r_p}$$

which is consistent with the assumptions of tubular pores and only axial diffusion.

5. The remaining general parameters and assumptions required for the calculations are listed below.

(*a*) Catalyst porosity, $\varepsilon_p = 0{\cdot}75$*

(*b*) Glucose concentration in venous blood, $C_{A_0} = 0{\cdot}5 \times 10^{-5}$ mol/cc

(*c*) Glucose diffusivity in plasma or pore $D_p = 0{\cdot}7 \times 10^{-5}$ cm^2/s

(*d*) Effective glucose diffusivity in membrane, $D_m = 0{\cdot}50 \times 10^{-5}$ cm^2/s.

Transport equation development

Zero-order reaction

The case of zero reaction order will be considered first. For this case, the total catalyst pore volume is simply glucose consumption, G, divided by the volume reaction rate:

$$V_p = \frac{G}{k_v}$$

The total electrode volume is

$$V_t = V_p/\varepsilon_p = G/k_v\varepsilon_p,$$

and the catalyst volume is

$$V_C = (1-\varepsilon_p)\, V_t = (1-\varepsilon_p)\, G/\varepsilon_p k_v.$$

The pore length, calculated below, is dependent on the mode of glucose transport. Once it has been determined, the projected area of the electrode (total membrane area) is simply $A = V_t/l$.

Pore length for diffusion alone (Case I)

In the pore

$$D_p \frac{d^2 C_A}{dx^2} = k_v, \tag{6}$$

the boundary conditions are

$$C_A(0) = C_{A_i};\ \left.\frac{dC_A}{dx}\right|_{x=l} = 0 \tag{7a}$$

with C_{A_i} evaluated from the utilization of the flux through the membrane:

$$A\varepsilon_m D_m \frac{C_{A_0} - C_{A_i}}{t} = A\varepsilon_p k_v l. \tag{7b}$$

* It seems unlikely that membranes showing filtration coefficients approaching the upper limit can be constructed with 50Å pore size.

* Close to the theoretical limit for tabular pores.

Integration of Equation (6) and substitution of conditions (7a) and (b) yields an expression for $C_A(x)$. Evaluating this at the end of the pore, where $C_A(l) = 0{\cdot}2\,C_{A_0}$, gives

$$l^2 + \left(\frac{2\,D_p\,t}{0{\cdot}8\,D_m}\right)l - \frac{0{\cdot}8\,C_{A_0}\,D_p}{0{\cdot}75\,k_v} = 0$$

or

$$= -\frac{D_p t}{0{\cdot}8\,D_m} + \sqrt{\left(\frac{D_p t}{0{\cdot}8\,D_m}\right)^2 + \frac{0{\cdot}8\,C_{A_0}\,D_p}{0{\cdot}75\,k_v}}. \tag{8}$$

Pore length with convection alone (Case II)

The pore length must be such that 80% of the glucose entering the pore is utilized. To maintain the downstream reservoir concentration,

$$k_v A_p\, l = 0{\cdot}80\,C_{A_0}\,U_m\,A_p$$

or:

$$l = \frac{0{\cdot}8\,C_{A_0}\,U_m}{k_v}. \tag{9}$$

Pore length with convection and diffusion (Case III)

The blood on the outside of the membrane forms a reservoir of constant glucose concentration, C_{A_0}. The combined diffusive and convective flux through the membrane can be written as $C_{0_m}U_m$.

If $y_m = C_{A_m}/C_{0_m}$; $z_m = x/t$; and $M = \dfrac{1}{Pe_m} = \dfrac{D_m}{U_m t}$,

the transport in the membrane is given by

$$-D_m\frac{dC_{A_m}}{dx} + U_m C_{A_m} = C_{0_m}U_m,$$

or

$$M\frac{dy_m}{dz} - y_m = -1 \tag{10}$$

where the first term results from the diffusive flux and the second from the convective flux.

The boundary condition is

$$y_m(0) = C_{A_0}/C_{0_m}. \tag{11}$$

The solution to Equation (10)

$$y_m = 1 - \left(1 - \frac{C_{A_0}}{C_{0_m}}\right)e^{z_m/M}. \tag{12}$$

In the pore the transport equation is

$$N\frac{d^2y}{dz^2} - \frac{dy}{dz} = K_1 \tag{13}$$

where

$$z = x/l;\ N = 1/Pe_p;\ y = C_A/C_{0_p};$$
$$K_1 = \frac{k_v l}{C_{0_p}\,U_p}. \tag{14}$$

The boundary conditions are

$$\frac{dy}{dz}(1) = 0;\ y(o) - N\frac{dy}{dz}(o) = 1. \tag{15}$$

The solution to Equation (13) is

$$y = K_1 N e^{-\frac{1-z}{N}} - K_1(z+N) + 1. \tag{16}$$

At the interface of the membrane and pore, conservation of glucose and plasma gives

$$A\varepsilon_m U_m C_{0_m} = A\varepsilon_\rho U_\rho C_{0_p}$$

and

$$A\varepsilon_m U_m = A\varepsilon_p U_p$$

or

$$C_{0_m} = C_{0_p} = C_0.$$

The concentration at the interface must be continuous; hence:

$$C_{A_m}(t) = C_A(0)$$

giving

$$y_m(1) = y(0) \tag{17}$$

or

$$1 - (1 - C_{A_0}/C_0)\,e^{1/M} = 1 - K_1 N(1 - e^{-1/N}). \tag{18}$$

In addition,

$$y(1) = \frac{0{\cdot}2\,C_{A_0}}{C_0} = 1 - K_1 = 1 - \frac{k_v l}{C_0 U_p}.$$

Evaluating C_0, we obtain

$$C_0 = \frac{k_v l + 0{\cdot}2 C_{A_0} U_p}{U_p}. \tag{19}$$

Then,

$$K_1 = \frac{k_v l}{k_v l + 0{\cdot}2 C_{A_0} U_p}. \tag{20}$$

Substituting Equation (20) into Equation (18) and rearranging

$$l = 0{\cdot}8\frac{U_p C_{A_0}}{k_v} + \frac{D}{U_p}e^{-1/M}(1-e^{-1/N}). \quad (21)$$

Equation (21) is solved by successive approximations for l.

First-order reaction (Case III)

For a first-order reaction rate only the case of flow with diffusion is considered. The solution for the concentration and flux in the membrane is the same as that for zero order

$$y_m(1) = 1-\left(1-\frac{C_{A_0}}{C_{0_m}}\right)e^{1/M}. \quad (22)$$

The differential equation for the concentration in the pore is

$$N\frac{d^2y}{dz^2} - \frac{dy}{dz} = K_2 y \quad (23)$$

with boundary conditions

$$N\frac{dy}{dz}\bigg|_{z=0} - y\bigg|_{z=0} = -1 \text{ and } \frac{dy}{dz}\bigg|_{z=1} = 0 \quad (24)$$

where y again is C_A/C_0. The C_0 can be thought of as a fictitious concentration at $z = -\infty$ so that the solution of Wehner and Wilhelm [18] for flow can be applied directly:

$$y = g_0 \exp\left(\frac{z}{2N}\right)\left\{(1+a)\exp\left[\frac{a(1-z)}{2N}\right] - (1-a)\exp\left[\frac{a(z-1)}{2N}\right]\right\} \quad (25)$$

where

$$g_0 = \frac{2}{(1+a)^2\exp\left(\frac{a}{2N}\right) - (1-a)^2\exp\left(\frac{-a}{2N}\right)} \quad (26)$$

and

$$a = \left(1+\frac{4Dk_v}{U_p{}^2}\right)^{\frac{1}{2}}. \quad (27)$$

Now,

$$y(1) = 2ag_0 e^{1/2N} = 0{\cdot}2\,C_{A_0}/C_0 \quad (28)$$

$$y(0) = y_m(1) = 1-\left(1-\frac{C_{A_0}}{C_0}\right)e^{1/M}. \quad (29)$$

Combining Equations (28) and (29) to eliminate C_0 and rearranging:

$$1-e^{1/M} = \frac{2(1-a)(re^{a/n}-1) - 20ae^{1/M}e^{\frac{1+a}{2N}}}{(1-a)^2(r^2e^{a/n}-1)} \quad (30)$$

where

$$r = \frac{1+a}{1-a}.$$

Equation (30) is solved by successive approximations for l. C_0 is then evaluated from Equation (28)

$$C_0 = \frac{C_{A_0}(r^2e^{a/n}-1)(1-a)^2}{20ae^{\frac{1+a}{2N}}}. \quad (31)$$

The electrode cross-sectional area must be such that

$$U_p C_0 A\varepsilon_p = G$$

or

$$A = \frac{G}{U_p C_0 \varepsilon_\rho} \quad (32)$$

and

$$V_t = Al. \quad (33)$$

Results and discussion

Solutions to the equations, showing the effects of the various parameters, are shown in graphical form in Figs. 2–6.

Dependence of area on mean pore radius

Fig. 2 shows a plot of projected electrode area against mean pore radius of the electrode for various membrane filtration coefficients, with $k_S = 10^{-11}$ mol/cm^2/s.

The mean pore radius considered is from 1·0 to 10^{-2} μm. The value 1·0 μm is a typical small-pore diameter in current gas-diffusion electrodes, whereas 10^{-2} μm (100 Å) is of the order of upper microcrystallite size of noble metal blacks. The minimum practical mean pore radius is probably about 10^{-5} cm (10^{-1} μm).

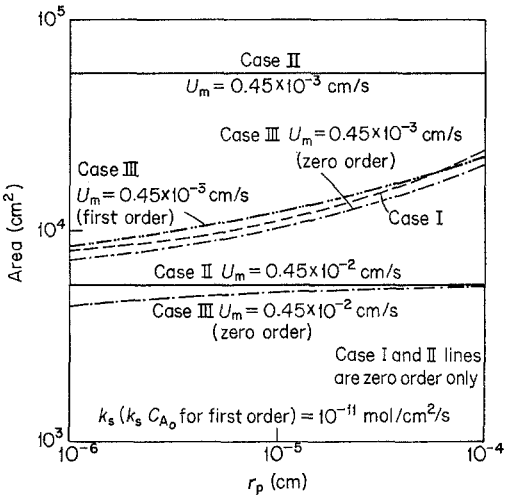

Fig. 2. Effect of electrode mean pore radius on membrane area.

It can be seen from Fig. 2 that the area for diffusion alone (Case I) is a function of pore radius and falls by a factor of approximately 2 (from 24,100 to 11,170 cm^2) with decrease in mean radius by one order of magnitude, from 10^{-4} to 10^{-5} cm. Area is independent of pore radius when only convection is considered, and is inversely proportional to U_m. For the largest values of U_m considered ($0{\cdot}45 \times 10^{-2}$ cm/s), area is 5,550 cm^2, and for the smallest values ($0{\cdot}45 \times 10^{-4}$ cm/s) area is 555,000 cm^2. It is of interest to note that the contribution of U_m term to the total flux is small, except when the highest value is considered ($0{\cdot}45 \times 10^{-2}$ cm/s). In each instance, Case III (diffusion plus convection) is always better than both diffusion alone (Case I), and convection alone (Case II). The values for Case III with $U_m = 0{\cdot}45 \times 10^{-4}$ cm/s are not plotted, but lie close to the Case I values (23,420 cm^2 compared with 24,100 cm^2 at $r_p = 10^{-4}$ cm; 11,000 cm^2 compared with 11,170 cm^2 at $r_p = 10^{-5}$ cm).

It is important to note that a major assumption was made in deriving the areas for Case I (diffusion alone), namely that no boundary layer was present at the blood-membrane interface. This is unrealistic in the general case, and is only justified if a sufficiently large convective flux is simultaneously present.

In practice therefore the highest attainable U_m values ($0{\cdot}45 \times 10^{-3}$ or better) are desirable when membrane areas are of the order of 20,580 cm^2 at $r_p = 10^{-4}$, falling by about 50% to 10,400 cm^2 at $r_p = 10^{-5}$. Larger values of U_m have the effect of causing proportionate area reductions.

Additional points for Case III have been plotted in Fig. 2 for the intermediate U_m value of $0{\cdot}45 \times 10^{-3}$, showing the effect of first-order kinetics on membrane area at $r_p = 10^{-5}$ cm.

At the larger value of r_p, area increases by about 9% to 22,520 cm^2 compared with the zero-order case. At $r_p = 10^{-5}$ cm, the increase is again small (about 8% to 12,100 cm^2).

Effect of U_m on area

Fig. 3 summarizes the effect of U_m on area at different values of r_p for Case II and Case III. At sufficiently small values of U_m, the $A - U_m$ curve at constant r_p for Case III tends to the area for diffusion alone. At sufficiently large values ($\sim 5 \times 10^{-3}$ cm/s), the family of curves for different values of k_v becomes asymptotic with the line corresponding to convection alone (Case II).

Again, points corresponding to the first-order case have been plotted for $U_m = 0{\cdot}45 \times 10^{-3}$, which show only small (8–11%) increases in area. At a lower convective flux value ($U_m = 0{\cdot}45 \times 10^{-4}$) area increases by approximately 50% over the zero-order case at the smallest r_p values considered (from 23,420 to 31,570 cm^2).

Effect of changing diffusional flux at constant U_m

In Fig. 4 the effect of membrane thickness variation at constant U_m is shown for r_p at the minimum practical value of 10^{-5} cm. The model

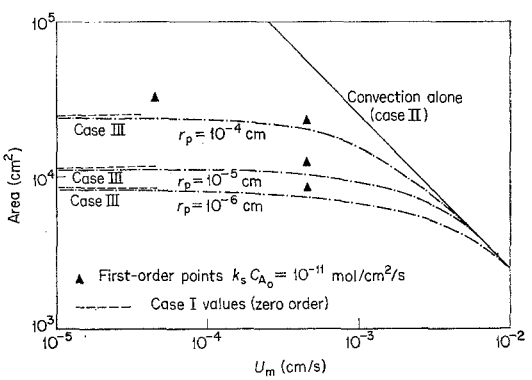

Fig. 3. Effect of convective velocity on membrane area, zero-order reaction ($k_s = 10^{-11}$ mol/cm^2/s.)

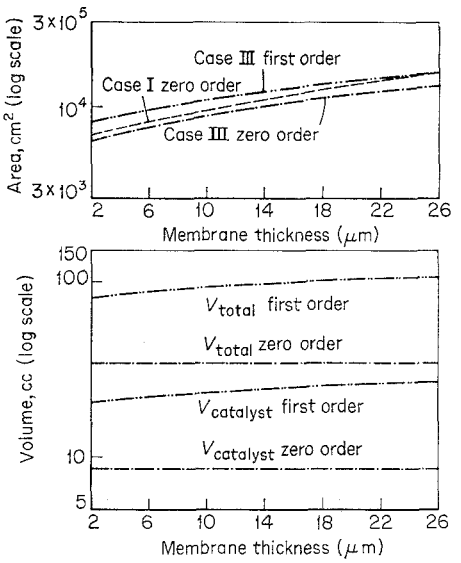

Fig. 4. Effect of membrane thickness at constant U_m (Dual-porosity Membrane), $r_p = 10^{-5}$ cm, $U_m = 0{\cdot}45 \times 10^{-3}$ cm/s, k_s ($k_s C_{A_0}$ for first order) $= 10^{-11}$ mol/cm²/s, Case III.

is presumed to represent a biporous membrane consisting of a thin small-pore (50 Å radius) region which provides the major flow resistance, together with a supporting region of larger pore size. Such a membrane is a possible answer to obtaining high U_m values in practice ($\sim 0{\cdot}45 \times 10^{-3}$ or better). In this model a 10-fold increase in thickness from 2·5 to 25 μm causes about 100% increase in area in Case III at zero order (from 6,550 to about 13,100 cm²). The same trend is shown by the results for the first-order case, which indicates an area requirement about 28% higher than zero order for the 2·5 μm membrane (8,390 cm²), and about 12% higher for the 25 μm membrane (to about 15,340 cm²).

Dependence of volume on thickness at constant filtration coefficient

This is also plotted for the lowest practical r_p value (10^{-5} cm) and for $U_m = 0{\cdot}45 \times 10^{-3}$ in Fig. 4.

At zero order for all cases considered, volume is independent of changing diffusional flux. However, for the first-order case an approximately 30% increase in volume occurs as membrane thickness is increased from 2·5 to 25 μm, when total electrode thickness is of the order of 3 times that for the zero-order case at 80% conversion (106 cc as opposed to 34 cc approximately). The total catalyst volume under first-order conditions is about 26·5 cc. This represents about 560 g for a metal the density of platinum and as such is only marginally acceptable for an implantable fuel cell.

For the zero-order case under the same conditions about 8·9 cc of catalyst would be required.

Effect of pore size on volume ($k_s = 10^{-11}$ *mol/cm²/s*, $U_m = 0{\cdot}45 \times 10^{-3}$)

Fig. 5 shows the relationship between pore size and electrode volume. At large r_p values (10^{-4} cm) catalyst volumes and weights become unacceptably high. As a practical lower limit of electrode thickness (pore length) is perhaps 25 μm, giving a total practical electrode volume of 26 cc for the zero-order case calculated for a biporous 15 μm membrane, with $U_m = 0{\cdot}45 \times 10^{-3}$, there is little point in attempting to construct electrodes with r_p less than about 10^{-5} cm

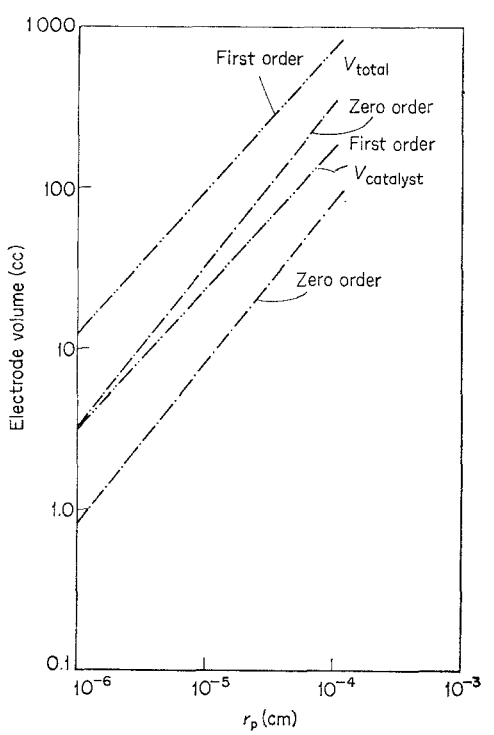

Fig. 5. Effect of pore size, r_p, on electrode volume, k_s ($k_s C_{A_0}$ for zero order) $= 10^{-11}$ mol/cm²/s, $U_m = 0{\cdot}45 \times 10^{-3}$ cm/s, Case III).

in this case. However, in the first-order case, the greater catalyst weight required necessitates an increase in k_v, which would be best carried out by increasing k_s.

Effect of variation of rate constant

Fig. 6 shows the effect of changing K_s on membrane area at various U_m values at $r_p = 10^{-5}$ cm. In addition, the diffusion case alone is shown, together with the first-order case for the largest practical value of U_m ($0{\cdot}45 \times 10^{-3}$ cm/s). This plot is analogous to Fig. 2, as both represent variations in k_v, one at constant k_s, the other at constant r_p. It can be seen that increase in k_s beyond the value of 10^{-11} mol/cm^2/s only marginally reduces area for all cases, though an order of magnitude reduction in k_s (from 10^{-11} to 10^{-12}) approximately doubles the membrane area required for the cases with U_m in the practical range.

In the same way, Fig. 5 may be used to show the variation in catalyst volume with k_s at constant r_p. It can be seen that reducing k_s by an order of magnitude at $r_p = 10^{-5}$ (equivalent to increasing r_p to 10^{-4} cm at $k_s = 10^{-11}$) results in catalyst volumes of 75 cc for the zero-order case and 180 cc for the first-order case. These represent weights of 1·6 and 3·8 kg, respectively, for a catalyst metal of the density of platinum,* and are thus entirely unacceptable for implantable use.

These considerations suggest that $k_s = 10^{-11}$ is the lowest practical limit in the zero-order case, with a slightly higher value ($k_s C_{A_0} \sim 3 \times 10^{-11}$) for the first-order case to keep the total catalyst weight at a reasonable level.

As the lower practical limits of electrode volume are probably about 25 cc for areas of 10,000 cm^2, there is little to be gained by going to catalysts that allow oxidation to proceed at rates substantially greater than $k_s = 10^{-11}$ ($k_s C_{A_0} \sim 3 \times 10^{-11}$ for the first-order case) though a fuel cell containing such a catalyst could operate more advantageously, as will be discussed in the next section.

* If catalysts of other types (for example, inorganic or organic semiconductors) can be developed for glucose oxidation, these weights would fall by approximately a factor of 10 for the same catalyst volume.

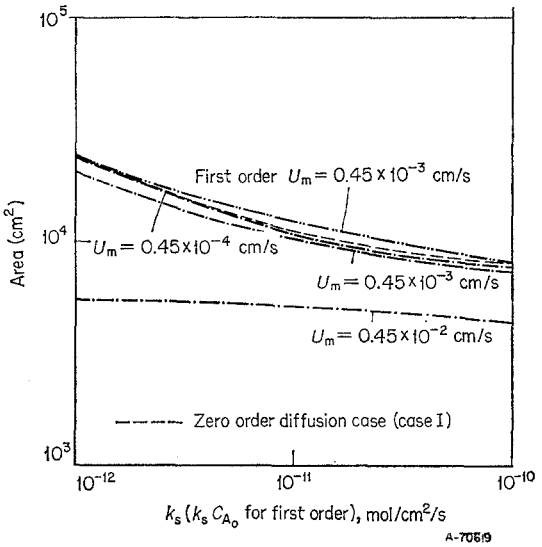

Fig. 6. Effect of surface rate constant, k_s, on membrane area ($r_p = 10^{-5}$ cm), Case III.

Conclusions

The results indicate that we should aim to use a membrane that allows a U_m value of $0{\cdot}45 \times 10^{-3}$ cm/s or better, as this is probably the smallest order-of-magnitude value that would reduce the thickness of the diffusion layer on the blood side of the membrane to acceptable limits. At a pressure head of 50 mmHg (70 cm H_2O), this corresponds to a filtration coefficient of about $3{\cdot}5 \times 10^{-6}$ cc/cm^2/cm H_2O/s. Such a figure is not attainable using commercially available membranes with the required pore-size, but should be obtainable using dual porosity membranes with a thin layer of small-pore (50 Å) material supported on a larger pore structure about 15 μm in thickness. For such a membrane, the area required (with $k_s = 10^{-11}$ mol/cm^2/s and $r_p = 10^{-5}$) would be about 11,000 cm^2 (zero order) or 12,500 cm^2 (first order). Corresponding electrode volumes (75% porosity) would be 35 and 75 cc respectively. Larger r_p or smaller k_s values will result in larger membrane areas and unacceptable catalyst weights. If first-order oxidation of glucose occurs, the catalyst weight (75 cc total electrode volume) is only marginally acceptable, and higher k_s values would be desirable (3×10^{-11} mol/cm^2/s). Practical considerations indicate that the minimum electrode thickness would be about 25 μm, corresponding to a total volume (at 11,000 cm^2 area) of 27·5 cc.

There is therefore little point in attempting to construct electrodes with a mean pore radius of less than 10^{-5} cm, which other considerations suggest is a limiting value. Larger k_s values than 10^{-11} (zero order) or 3×10^{-11} (first order), or alternatively a thicker electrode if low-density catalysts became available, together with larger areas, will be required to provide an adequate safety margin and to account for the tortuosity of practical electrodes. Bearing this in mind, the minimum requirement for a practical 4·5 W unit would be:

(1) $U_m = 0{\cdot}45\times10^{-3}$ mol/cm^2/s.
(2) $r_p = 10^{-5}$ (or less).
(3) Area 11,000 cm^2 (zero order) or 12,500 cm^2 (first order).
(4) $k_s = 10^{-11}$ (zero order) or $k_s\, C_{A_0} = 3\times10^{-11}$ (first order) mol/cm^2/s.

It is important to point out that the above calculations are conservative in that they assume only two electrons are obtainable from the oxidation of glucose, with glucose acid as product, instead of the theoretical 24 (giving CO_2). There is evidence that gluconic acid is oxidized to CO_2 at the potentials considered in this paper. If this is practically possible and if we use the same available current density per geometric cm^2 as before (on Pt-Ru alloys or rhodium), the value of the glucose utilization falls by a factor of 12. At the same time k_s falls by the same amount from Equation (5).

Thus from Equation (5) and Fig. 6, the membrane area falls approximately a factor of 6 to 1850 cm^2 for the above parameters for complete oxidation of glucose to CO_2 under zero-order oxidation conditions. The volume of the electrode remains the same as before, with electrode thickness 180 μm for the zero-order case. Similarly, for the first-order case with $k_s\, C_{A_0} = 10^{-11}$, the area becomes about 1900 cm^2 with an electrode thickness of 350 μm under these conditions.

The membrane flow values and areas involved are thus of a reasonable order of magnitude. The same may be said to be true of the k_s values. The minimum value of the latter quantity considered (real current density 2×10^{-7} A cm^2 at 400 mV overpotential) corresponds from Equation (3) to an exchange current of only about 10^{-10} A/cm^2 for glucose oxidation. This is a modest value, of the same order of magnitude as that for oxygen reduction in dilute acid at room temperature.

Acknowledgment

The authors wish to acknowledge the support of the Institute of Gas Technology in-house basic research programme and helpful discussions with Dr. S. K. Wolfson, Jr., of the Michael Reese Hospital and Medical Center, Chicago.

Nomenclature

A	Area
C_A	Concentration of glucose
C_0	Total flux reference concentration
D	Diffusivity
F	Faraday's constant
G	Glucose conversion rate
i	Current density
K_1	Dimensionless rate constant, zero-order reaction
K_2	Dimensionless rate constant, first order reaction
k	Rate constant
k_s	Surface-based rate constant
k_v	Volume-based rate constant
l	Pore length
M	$1/Pe_m$
m	Reaction order
N	$1Pe_p$
n	Number of electrons in overall reaction
Pe	Mass transfer Peclet number
R	Gas constant
r	Radius
T	Temperature
t	Time, membrane thickness
U	Velocity
V	Potential, Volts
V_c	Catalyst volume
V_p	Pore volume
V_t	Total volume of electrode
x	Axial distance
y	Reduced concentration, C_A/C_O
Z	Dimensionless axial distance

Subscripts

i	interface

m membrane, or in membrane pore
o initial condition
p pore, or in pore

Greek letters

α Electrochemical transfer coefficient
ε porosity

References

[1] 'Artificial Heart Devices and Systems: A Conceptual Phase Study', Contract No. PH 43-65-1058, Stanford Research Institute (January 1966).

[2] F. N. Huffman, R. J. Harvey, and S. S. Kitrilakis, 'Design of an Implantable, Rankine-Cycle, Radioisotope Power Source'. Paper presented at the *Intersociety Energy Conversion Engineering Conference*, Miami Beach, Florida (August 1967) p. 750.

[3] M. Beltzer, *J. Electrochem. Soc.*, **114** (1967) 1200.

[4] R. F. Drake, 'Implantable Fuel Cell For an Artificial Heart', *Proc. The Artificial Heart Program Conference*, Washington, D.C. (June 1969) p. 869.

[5] J. Batzold and M. Beltzer, 'Feasibility Studies—Implantable Biological Fuel Cell', *ibid.*, p. 817.

[6] A. Kozawa, V. E. Zilionis, R. J. Brodd, and R. A. Powers, 'Search For a Specific Catalyst for Electrochemical Oxygen Reduction In Neutral NaCl Solution', *ibid.*, p. 849.

[7] 'Second Annual Summary Report: Implantable Fuel Cell For An Artificial Heart', Contract No. PH 43-66-976, Monsanto Research Corporation, (July 1968).

[8] A. J. Appleby, D. Y. C. Ng, S. K. Wolfson, Jr., and H. Weinstein, 'An Implantable Biological Fuel Cell With An Air-Breathing Cathode', *Proc. 4th Intersociety Energy Conversion Engineering Conference*, Washington, D.C. (September 1969) p. 346.

[9] J. O'M. Bockris, B. J. Piersma and E. Gileadi, *Electrochim. Acta*, **9** (1964) 1329.

[10] M. L. B. Rao, and R. G. Drake, *J. Electrochem. Soc.*, **116** (1969) 334.

[11] W. J. Latimer, 'Oxidation Potentials', 2nd ed., Prentice Hall, New York (1952) p. 128.

[12] C. W. Mansfield, 'Oxidation and Reduction Potentials of Organic Systems', Williams and Wilkins Co., Baltimore (1960).

[13] A. J. Appleby and C. Van Drunen, *J. Electrochem. Soc.*, **118** (1971) 95.

[14] S. J. Yao, A. J. Appleby, A. Geisel, H. R. Cash, and S. K. Wolfson, Jr., *Nature*, **224** (1969) 921.

[15] J. O'M. Bockris and H. Wroblowa, *J. Electroanal. Chem.*, **7** (1964) 428.

[16] A. T. Kuhn, H. Wroblowa, and J. O'M. Bockris, *Trans. Faraday Soc.*, **63** (1967) 1458.

[17] J. R. Pappenheimer and E. J. Landis, in 'Handbook of Physiology', Vol. II., p. 961–1034, P. Dow, Editor, American Physiological Society, Washington, D.C. (1963).

[18] J. F. Wehner and R. H. Wilhelm, *Chem. Eng. Sci.*, **6** (1956) 89.